Monte Carlo estimation of the absorbed dose in computed tomography

Jinwoo Kim [a], Hanbean Youn[b,c], Ho Kyung Kim [a,c*]
[a]*School of Mechanical Engineering, Pusan National University, Busan 46241, South Korea*
[b]*Department of Radiation Oncology, Pusan National University Yangsan Hospital, Yangsan, Gyeongsangnam-do 47011, South Korea*
[c]*Center for Advanced Medical Engineering, Pusan National University, Busan 46241, South Korea*
[*]*Corresponding author: hokyung@pusan.ac.kr*

1. Introduction

Assessment of patient dose in computed tomography (CT) at the population level has become a subject of public attention and concern, and ultimate CT quality assurance and dose optimization have the goal of reducing radiation-induced cancer risks in the examined population.[1] However, the conventional CT dose index (CTDI) concept is not a surrogate of risk but it has rather been designed to measure an average central dose.[2] In addition, the CTDI or the dose-length product has showed troubles for helical CT with a wider beam collimation.[3-5]

The purpose of this study is to devise an algorithm calculating absorbed dose distributions of patients based on Monte Carlo (MC) methods, and which includes the dose estimations due to primary and secondary (scattered) x-ray photons.

2. Materials and Methods

For numerical chest and head phantoms, as shown in Fig. 1, MC simulations using the Monte Carlo N-Particle transport code (MCNP version 5, RSICC, Oak Ridge, TN, USA) were performed. The small cone-angle beam geometry with a source-to-axis of rotation distance (d_{SA}) of 100 cm. The dimensions of the two phantoms were based on the conventional CTDI phantoms, of which outer diameters were 320 and 160 mm, respectively. Water was assumed as base material. To consider inhomogeneities of human anatomy, the chest phantom included two circular lung regions with a reduced density of water (0.2 $g.cm^{-3}$) and the head phantom was surrounded by $CaCO_3$ (2.7 $g.cm^{-3}$) to mimic cranial bones.

To compute the dose map from MCNP output data, every particle tracking (PTRAC) data set such as interaction type, location, and absorbed energy was categorized by primary and secondary x-ray photons and absorbed energy was accumulated to the interaction location of the photons for each primary and scattered dose data by using MATLAB R2015a (MathWorks Inc., Natick, MA, USA).

As shown in Fig. 2, dose due to primary photons includes the photoelectric interaction after a single Rayleigh scattering. And the Compton scattering can deposit energy partially at the sites, where the scattering is occurred, and the remainder at the site where further photoelectric interactions occur. Thus, the scattered x-ray photons are categorized into the first scattering and higher-order multiple scatterings, and for each scattered x-ray photon, partial energy deposition at Compton-scattering sites and the remaining energy deposition at remote photoelectric-interaction sites are separately categorized.

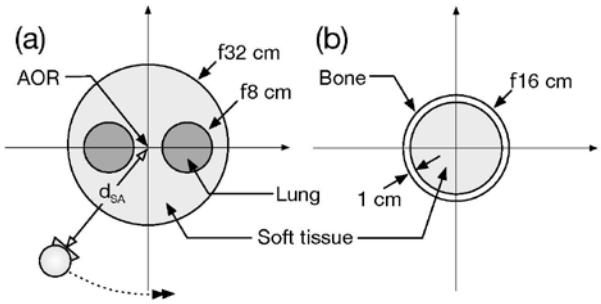

Figure 1. Numerical phantoms used for Monte Carlo simulations: (a) chest and (b) head phantoms

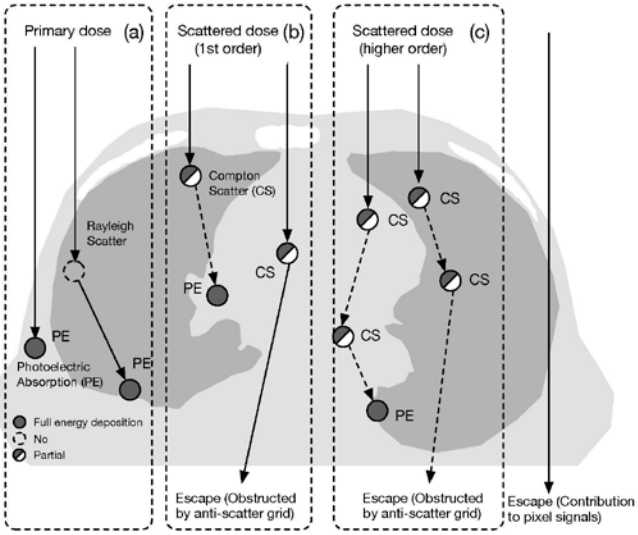

Figure 2. X-ray photon interactions considered in this study for dose calculations.

3. Preliminary Results

Fig. 3 shows the spatial dose distributions in the central slices of chest phantoms due to primary, first-order scattering, higher-order scattering and total interactions. The results obtained from the MC methods were normalized by number of histories.

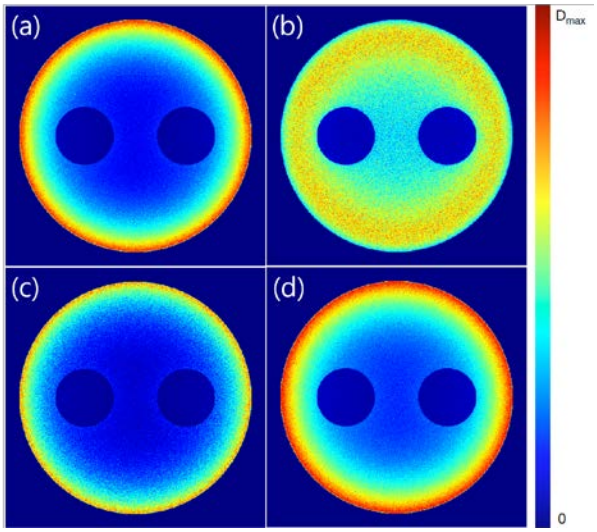

Figure 3. Calculated dose distributions in the central slices of chest phantoms: (a) single-scattering, (b) higher-order multiple scattering, (c) primary and (d) total dose distribution.

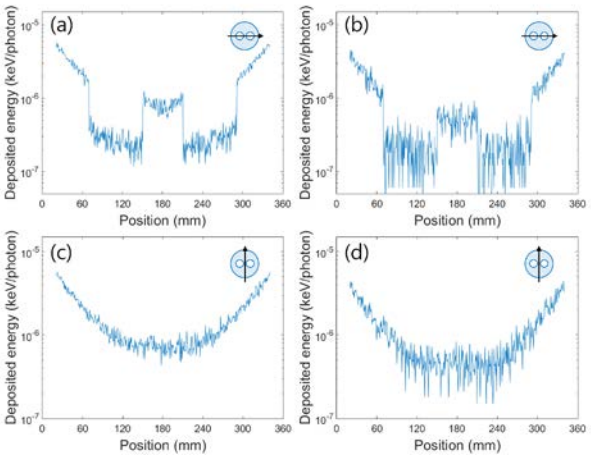

Figure 4. Extracted dose profiles from Fig. 3: (a) horizontal direction single-scattering, (b) horizontal direction primary, (c) vertical direction single-scattering, (d) vertical direction primary profile.

For more quantitative analysis, profiles extracted from Fig. 3 are shown in Fig. 4. In these figures, only single-scattering and primary events were considered and logarithmic scale was applied.

Similarly, Fig. 5 shows the spatial dose distributions in the central slices of head phantoms due to primary and scatter interactions. Profiles extracted from Fig. 5 are shown in Fig. 6. In the same manner, only singe-scattering and primary events were considered and logarithmic scale was applied.

4. Conclusions

Simple algorithms to estimate a patient specific CT dose based on the MCNP output data have been introduced. For numerical chest and head phantoms, the spatial dose distributions were calculated. The results were reasonable.

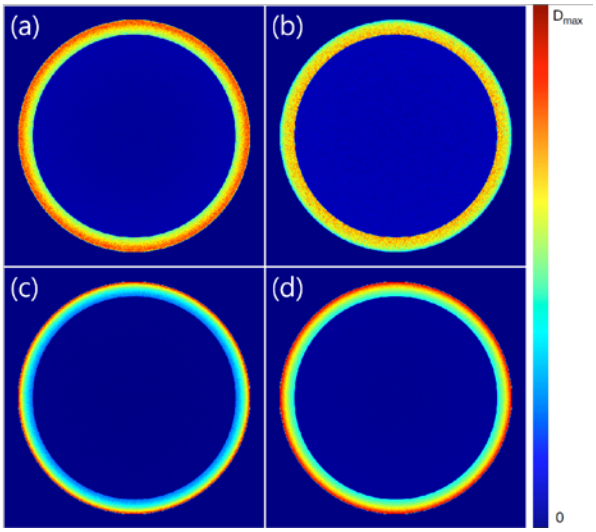

Figure 5. Calculated dose distributions in the central slices of head phantoms: (a) single-scattering, (b) higher-order multiple scattering, (c) primary and (d) total dose distribution.

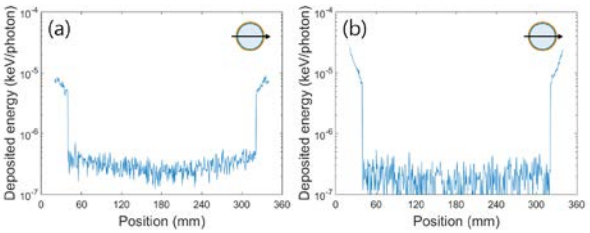

Fig. 6. Extracted dose profiles from Fig. 5: (a) single-scattering, (b) primary profile.

The estimated dose distribution map can be readily converted into the effective dose. The important list for further studies includes the validation of the models with the experimental measurements and the acceleration of algorithms.

ACKNOWLEDGEMENT

This work was supported by the research grant funded by the Samsung Electronics Co. and by the National Research Foundation of Korea (NRF) grant funded by the Korean Government (MSIP) (No. 2013M2A2A9046313).

REFERENCES

[1] D. J. Brenner and E. J. Hall, "Computed tomography – An increasing source of radiation exposure," New Engl. J. Med. **357**(22), pp. 2277-2284, 2007.
[2] D. J. Brenner, "Is it time to retire the CTDI for CT quality assurance and dose optimization?," Med. Phys. **32**(10), pp. 3225-3226, 2005.
[3] R. L. Dixon, "A new look at CT dose measurement: Beyond CTDI," Med, Phys. **30**(6), pp. 1272-1280, 2003.
[4] J. M. Boone, "The trouble with $CTDI_{100}$," Med. Phys. **34**(4), pp. 1364-1371, 2007.
[5] R. L. Dixon and J. M. Boone, "Stationary table CT dosimetry and anomalous scanner-reported values of $CTDI_{vol}$," Med. Phys. **41**(1), p. 011907, 2014.